6

Light Emitting Diode and UV Photodetector Characteristics of Solution Processed n-ZnO nanorods/p-Si Heterostructures

6.1 Introduction

Over the years, optoelectronic devices have attracted attention from the scientific community to use it in different applications. Devices such as UV photodetector and LEDs are widely studied by using different semiconducting materials in different homojunctions and heterojunction configurations. UV detectors are required in variety of applications such as pollution monitoring, military applications, water sterilization, biomedical applications and secure space communications etc. These applications require a highly sensitivity device with fast response/recovery and high signal to noise ratio. Mainly silicon based devices are dominating the industry for such applications owing to its fast response and high S/N ratio. However, these devices suffer from limitations such as need of additional filters to remover IR and visible light, need of high voltage operations, degradation, ultra-high vacuum requirement and degradation of devices (Liu et al., 2010). Wide band gap compound semiconductors are considered to be a better substitute for silicon based UV photodetector owing to its visible blindness and have ability to thermal and chemical stability, suitable to work in harsh environmental conditions. Wide bandgap materials have attracted considerable attention for LEDs fabrication and are used in several applications like displays, automobiles and illumination devices.

The bandgap of ZnO which lies in UV region makes it suitable candidate for UV photodetector applications. Apart from that, binding energy of exciton is ~ 60 meV which is much higher in comparison to other wide band gap semiconductor and is also greater than the room temperature thermal energy (25 meV). These unique and robust traits of ZnO makes it a suitable candidate for UV based optoelectronic applications (Pearton et al., 2005)(Ü Özgür et al., 2005b). UV based optoelectronic devices are fabricated and performance of these devices are dependent on type of deposition technique and morphology. ZnO based nanorods have high surface to volume ratio, hence shows enhanced optoelectronic properties because of its large surface states. ZnO based UV photodetectors are synthesized in MIM as well as p-n junction configuration. Presence of intrinsic point defect i.e. oxygen vacancies/zinc interstitial makes ZnO n-type conducting. Fabrication of p-ZnO is still a challenging process as described in chapter 5 (W. I. Park et al., 2002)(W. Il Park et al., 2002). Hence, a different p-type substrate is employed to achieve p-n junction with n-ZnO. Substrates such as silicon, silicon carbide, and GaN are used with ZnO to synthesize devices. Silicon substrates are relatively cheaper and are easily available in comparison to other substrates i.e. GaN and SiC. Also, it is easy to integrated silicon based devices in IC industries hence making it a suitable candidate for optoelectronic industries (Al-Hardan et al., 2014). Hence, n-ZnO in conjunction with silicon is widely used by research community for variety of applications. UV photodiode is prepared by Lei et. al. using thermally deposited n-ZnO on p-Si heterojunction (Luo et al., 2006). The devices showed 0.07 A/W responsivity at 20 V reverse bias voltage under illumination of 365 nm UV radiation.

In this chapter, we discuss the UV sensing and derived light emitting characteristics of a solution derived n-ZnO nanorods/p-type Si substrate (100) heterojunction devices. This chapter will analyse the physical and electronic properties of these heterostructures. The UV sensing and PL derived light emission properties are also investigated for the fabricated devices.

6.2 Experimental Details

ZnO nanorods are deposited on 1 cm x 1 cm (100) p-Si wafer by a simple chemical bath deposition technique (Kumari and Dixit, 2019). Prior to deposition, the substrate is cleaned by ultra-sonicating subsequently in acetone, IPA and DI water for 15 minutes. Further, the cleaned substrates are dipped in dilute 10% HF solution to remove any oxide layers for 1 minute, followed by rinsing with DI water. The seed layer is first deposited on the silicon substrate to enable the growth of nanorods, described in previous chapter. Further, nanorods are deposited by putting the seeded substrate upside down in aqueous and equimolar (25 mM) solution of zinc nitrate hexahydrate ($Zn(NO_3)_2 \cdot 6H_2O$) and methenamine ($C_6H_{12}N_4$) . The solution was stirred at room temperature for an hour prior to putting the substrate in the solution. This solution containing substrate is then put in an oven for 6 hours at 93°C. The further crystallization process is similar as described in last chapter.

6.3 Results and discussion

6.3.1 Structural and Microstructural Properties

Structural analysis of the samples is investigated using powder XRD system. The diffraction pattern of the ZnO nanorods is presented in figure 6.1 (a). All XRD peaks matched well with hexagonal wurtzite structure (ICDD #. 036-1451). The XRD results indicate the synthesis of pure phase ZnO. The ZnO nanorods have a preferred orientation along (002) plane substantiating its C-axis orientation. Presence of other diffraction peaks suggests the polycrystalline nature of nanorods. Higher intensity towards (002) plane indicates enhanced texture along C-axis. The estimated lattice parameters a and c are 5.207 Å and 3.18 Å, respectively. The calculated crystallite size along (002) plane is 23.48 nm.

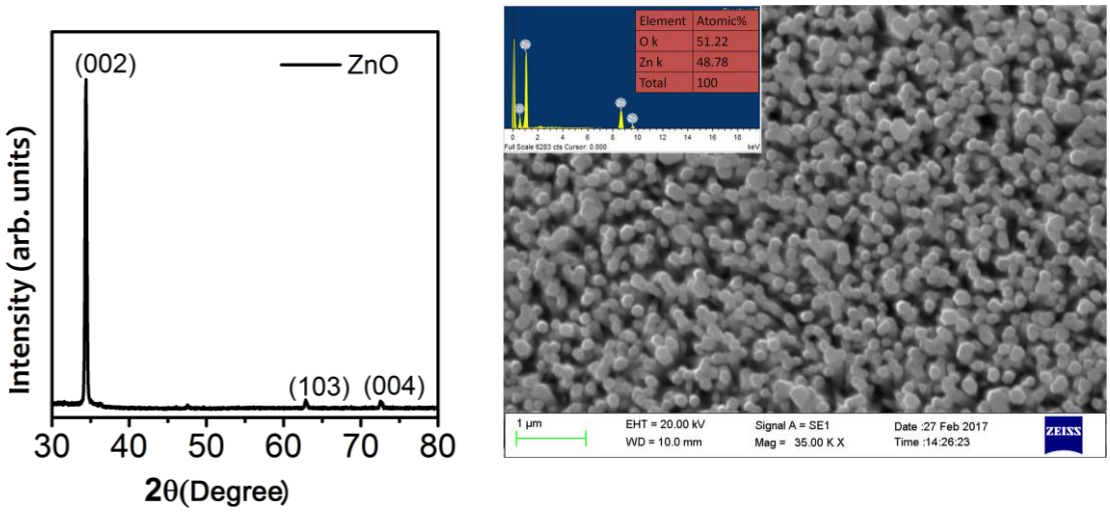

Figure 6.1 : (a) XRD of ZnO nanorods and (b) Top view of ZnO nanorods with EDS data in inset

The estimated values matched well with the reported value of ZnO nanorods. Morphological information of the sample is calculated by SEM and AFM analysis. The SEM results showed highly oriented ZnO nanorods with diameter 120 nm ± 5 nm. The image also substantiates uniform distribution of nanorods along the surface of the film. Hexagonal top is observed in the planar view of grown ZnO nanorods, figure 6.1 (b). The EDS analysis suggests that nearly stoichiometric atomic compositions of zinc and oxygen atoms with atomic fractions ~ 49% ± 5% and ~ 51% ± 5%, respectively, inset figure 6.2 (a). The topographical image of AFM analysis further confirmed the nanorods formation, figure 6.2 (a). The estimated RMS and average roughness of the nanorods are ~40 nm and ~33 nm, respectively.

6.3.2 Optical Properties

DRS experiment is performed on the sample to estimate the band gap. Further, Tauc plot is used to plot the graph between $(\alpha h\nu)^2$ and energy, where intercept depicts the band gap and the estimated band gap is 3.26 eV, figure 6.2 (b).

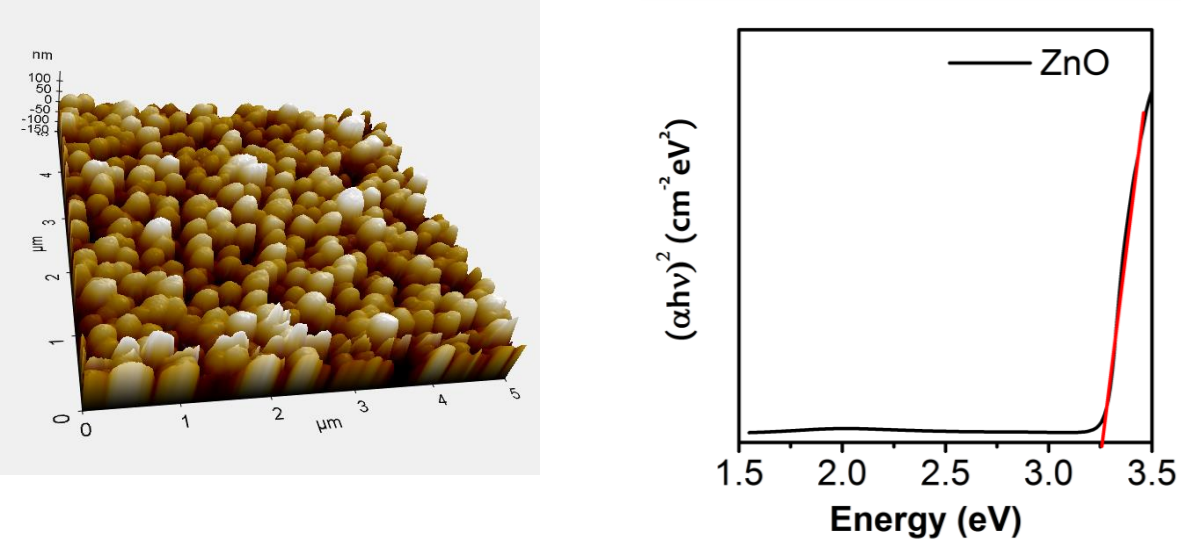

Figure 6.2: (a) AFM image of ZnO nanorods and (b) Calculated band gap of ZnO

The room temperature PL is performed to investigate the defect levels as well as light emitting properties of grown nanorods, given in Fig. 6.3 (a).

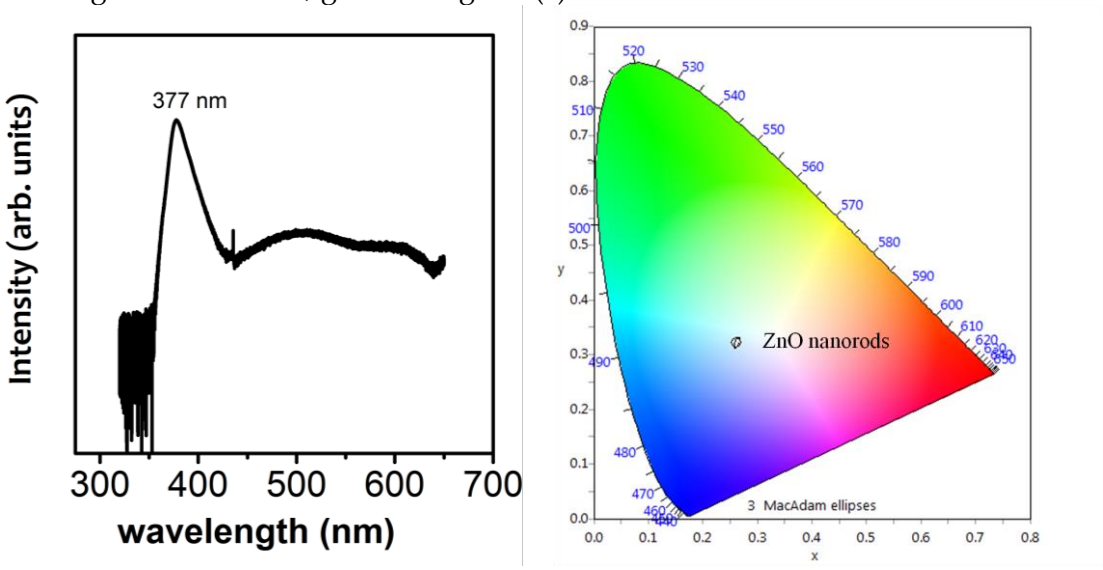

Figure 6.3: (a) Photoluminescence of ZnO nanorods and (b) Color co-ordinates of nanorods

These ZnO nanorods exhibits an intense peak at 377 nm which is attributed to band to band radiative recombination of excitons, substantiating band gap around 3.29 eV which is relatively higher than calculated absorption band edge from optical spectroscopic measurements.

Another relatively low and narrow peak is detected at 435.5 nm (~2.8 eV) which is assigned to presence of zinc interstitials. This blue emission is attributed to zinc interstitials. A broad and weak peak is also observed in visible wavelength region which is accredited to different point defects present in ZnO nanorods (Djurišić et al., 2004). The estimated ratio of NBE/DLE is ~75.3 which is high and substantiates reasonable optical quality of nanorods. The color of light emission of the nanorods is understood by using a CIE 1931 color calculator. The PL spectrum is transported in the software to understand the color coordinates generated by the sample. The estimated color coordinates of the sample is observed near to light blue region, figure 6.3 (b). The combined effect of all the emission is converted into light blue emission.

6.3.3 Current-Voltage Characteristics

Electrical measurements are performed by depositing top and bottom circular silver contact with diameter ~1 mm on n-ZnO and p-Si, inset of figure 6.4 (a). I–V measurements are carried out in -5 V to 5 V sweep DC voltage under dark and UV light (365 nm), shown in Fig 6.4 (a). The current increases in accordance with sweep voltage along forward bias and blocking of current is observed in reverse bias, substantiating diode behaviour of n-ZnO/p-Si diode. Under dark, the heterojunction showed rectifying diode behaviour with turn on voltage ~1.1 V. The estimated rectification ratio of this p–n heterostructure is ~200. This result substantiates the formation of p-n junction between p-Si and n-ZnO. Under UV radiation, increase in current is observed from 0.2 mA to 1 mA substantiating UV sensing behaviour of ZnO. The devices showed change in color under dark and UV conditions which is given in the inset of figure 6.4 (b). Under UV light, device emitted blue color which is in accordance with the results of CIE color calculator.

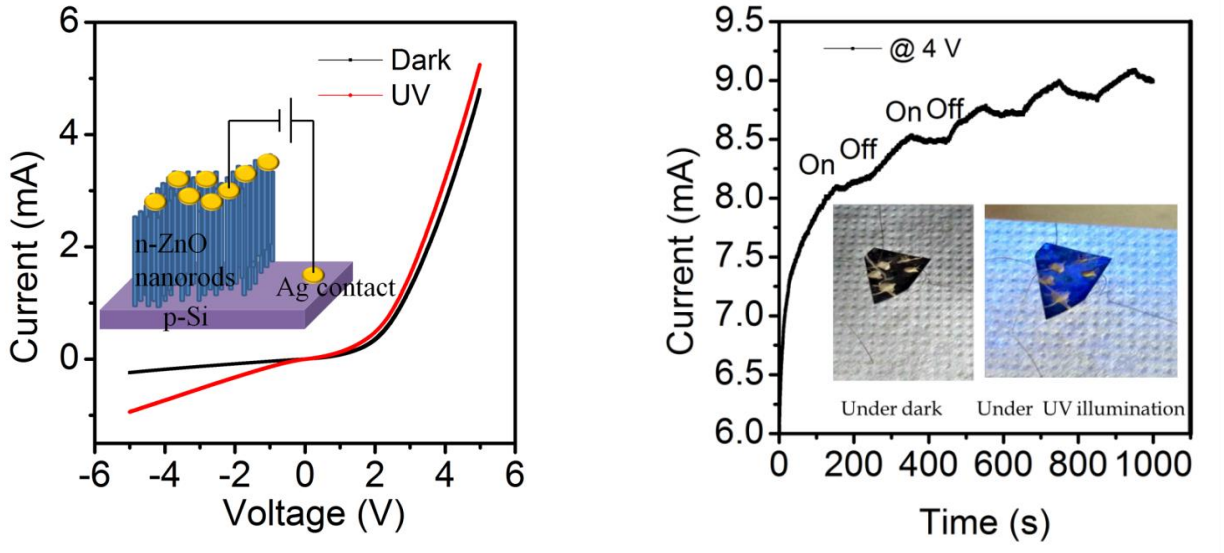

Figure 6.4: (a) I-V curve of heterojunction and (b) Emitted color of the junction under dark and UV

Further, UV switching behaviour is obtained by turning the UV light on and off at 4 V in a given time range. The obtained response is presented in figure 6.4 (b). It is evident from the figure that the current is not able to return to its original position after turning off the UV light.

This might be due to carrier trapping in defect states. However, it showed sequential increase in current when UV is on and decrease in current when UV light is off.

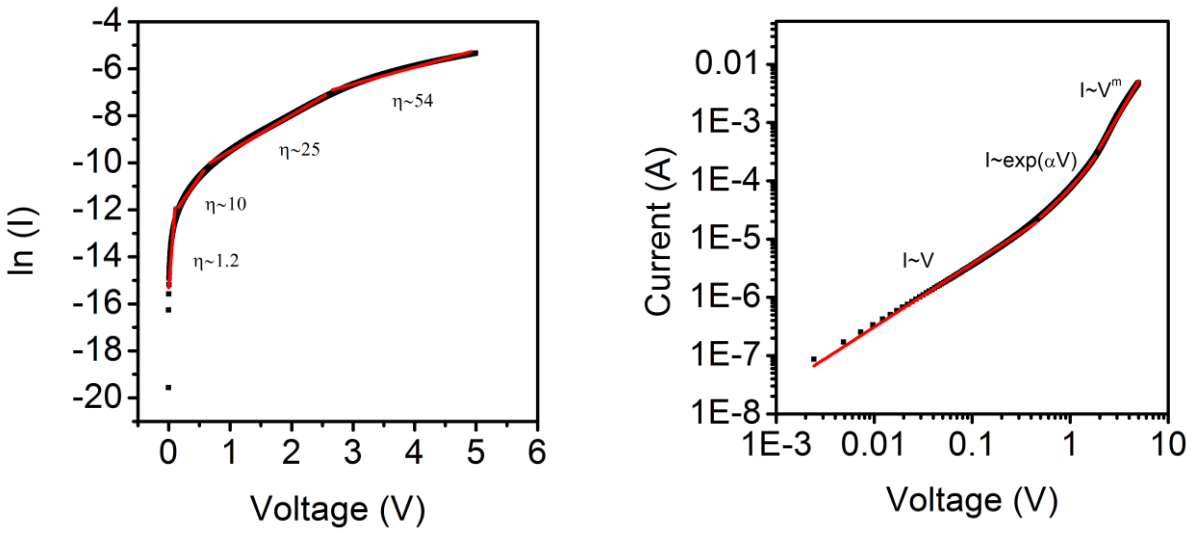

Figure 6.5: (a) Semilogrithmic curve of I-V and (b) log-log curve of I-V

The quality of synthesized diode is measured by measuring its ideality factor η. The value of η (~1 in lower voltage, ~2 in higher voltage region) indicates the variation of the diode from ideal behaviour. Semilogrithmic graph is plotted between current and voltage, figure 6.5 (a) and the slop is used to calculate η value. It is evident from the graph that η~ 1 in lower voltage region (~0.5 V) however, in higher voltage region the diode is highly non-linear. This nonlinearity is higher region is attributed to defects present in ZnO nanorods. The current conduction mechanism is investigated by plotting log-log current and voltage characteristics, figure 6.5 (b). The curve is divided into three regions representing three conduction mechanisms. At lower voltage, the current is proportional to voltage substantiating tunnelling mechanism for current conduction. The next region, the current follows exponential law, indicating tunnelling recombination current conduction. Finally the third region follows power law relation between current and voltage, pointing SCLC conduction mechanism.

6.4 Conclusion

In summary, we have synthesized n-ZnO nanorods/p-Si heterojunction devices using a simple hydrothermal process. The XRD analysis of the nanorods substantiates the formation of phase pure c-axis oriented polycrystalline ZnO. SEM and AFM measurements indicate the formation of vertically aligned and uniformly distributed nanorods, diameter ~120 nm. EDS analysis indicates equal atomic fractions of zinc and oxygen atoms. The calculated band gap by using DRS UV-Vis measurement is ~3.26 eV. PL spectrum indicated that the fabricated devices exhibits NBE emission in conjunction with defect emission, suggesting ZnO has potential in optoelectronic device applications, especially UV PDs and LEDs. The observed color spectrum of the devices showed a blue light emission, further substantiated by CIE color calculator coordinates. Rectifying diode like behaviour is observed in n-ZnO/p-Si device as indicated by I-V measurements. Substantial increase in current is observed in reverse bias of diode under UV illumination, substantiating its UV sensor properties. UV photodetector characteristics are shown by noticing the change in current and change in sample's color. Thus, these heterosturctures may be used as UV LEDs. However, LED properties can be further investigated using electroluminescence (EL) studies.